

# Systematic Theoretical Study of Structures and Bondings of the Charge-Transfer Complexes of Ammonia with HX, XY, and X<sub>2</sub> (X and Y are Halogens)

Yong Zhang, Cun-Yuan Zhao, and Xiao-Zeng You\*

Coordination Chemistry Institute, State Key Laboratory of Coordination Chemistry, Nanjing University, Center for Advanced Studies in Science and Technology of Microstructures, Nanjing 210093, PRC

Received: September 24, 1996; In Final Form: December 13, 1996<sup>⊗</sup>

The hybrid Hartree–Fock density functional theory (HF-DFT) method was employed with the combined use of CEP-121G(d,p) for H, N, F, and Cl, and RCEP(d) for Br and I to produce the equilibrium structures for both component molecules and the title charge-transfer (CT) complexes. Results are close to experimental data. The intermolecular stretching force constant  $k$  derived from the parabolic fit of its energy curve is parallel to the experimental value. The excellent linear relationship between the calculated  $k$  and the binding energy  $E_B$  shows the consistency of the present work in describing the intermolecular bonding intensity. The *step-by-step charge-transfer* model was proposed to directly evaluate the extent of intra- and intermolecular CT. The intermolecular CT amount,  $\delta_1$ , is not large, in accordance with the weak bonding in the complex. But the CT effect is found to be significant in determining the bonding strength.  $\delta_1$  is parallel to the dipole moment of the complex. The change of the total dipole moment in the complex formation can be used in the quantitative assessment of the electrostatic and nonelectrostatic contributions of the intermolecular bonding.

## I. Introduction

Owing to the simplicity and familiarity of the components in chemistry, a series of gas-phase charge-transfer (CT) complexes H<sub>3</sub>N·AB (AB can be HX, XY, or X<sub>2</sub>, where X or Y is a halogen) have been the recent focus of a lot of chemical work.<sup>1–5</sup> The structure and bonding nature of these supermolecules are of particular interest. Their gas-phase structural information can be experimentally obtained through the analysis of the ground-state rotational spectrum observed by pulsed-nozzle Fourier transform microwave spectroscopy.<sup>4</sup> The charge-transfer extent can be reflected by the nuclear quadrupole hyperfine structure because it can affect the quadrupole coupling constants of halogens with quadrupolar nuclei. The intermolecular stretching force constant,  $k$ , can be obtained experimentally on the basis of known rotational constants and the centrifugal distortion constants.<sup>6</sup> It can be used to quantitatively evaluate the interaction strength. Therefore, the CT effect and the bonding nature of these complexes can be investigated well by experimentation. If significant charge transfer happens during the formation of this kind of complex, the structural changes of the subunits, the binding energy, and the intermolecular stretching force constant associated with such a process must be large. Meanwhile, the dipole moment of the complex must be great as well.

A theory involving resonance between the no-bond structure (corresponding to  $\psi_0(\text{D,A})$ ) and the dative structure (corresponding to  $\psi_1(\text{D}^+-\text{A}^-)$ ) was proposed by Mulliken<sup>7</sup> in the theoretical study. In that formalism, the ground-state wave function is approximately expressed as follows:<sup>8</sup>

$$\psi_N = a\psi_0(\text{D,A}) + b\psi_1(\text{D}^+-\text{A}^-) \quad (1)$$

As a matter of fact, the no-bond wave function has the covalent bonding character, and the dative wave function has the ionic bonding character,<sup>8</sup> so  $\psi_0(\text{D,A})$  and  $\psi_1(\text{D}^+-\text{A}^-)$  may also be regarded as the covalent and ionic parts of the whole ground-state wave function. Since the interaction in an ionic bond is

electrostatic in nature, the coefficients  $a$  and  $b$  can be used in the evaluation of the weights of electrostatic and nonelectrostatic contributions to the intermolecular bonding between two subunits. The CT effect was used to explain the properties of these complexes of lone-pair donors and halogens or other halogen-containing acceptors.<sup>9</sup> It was found that the CT force was the overwhelming factor in the determination of the complex stability in the cases of strong  $n \rightarrow \sigma$  and  $n \rightarrow v$  complexes. However, the consideration of only the charge-transfer interaction may not be sufficient in describing the ground-state stabilization in some complexes.<sup>10</sup> The Coulombic interaction was considered as the main origin in the complexes of H<sub>3</sub>N·F<sub>2</sub>, H<sub>3</sub>N·Cl<sub>2</sub>, and H<sub>3</sub>N·ClF.<sup>11</sup> A recent experimental study<sup>4</sup> on the similar supramolecular compound H<sub>3</sub>N·BrCl has suggested the electrostatic origin of the intermolecular interaction with probably only a small amount of the intermolecular charge redistribution during the formation of the complex. The *ab initio* research<sup>12</sup> on the hydrogen-bonded complexes, i.e., H<sub>3</sub>N·HCl and H<sub>3</sub>N·HBr, showed that they prefer the neutral type to the ionic type. In fact, the hydrogen bond was classified as the  $n \rightarrow \sigma^*$  type in which the CT effect was thought to be the dominant factor to determine the supramolecular structure.<sup>13</sup>

The common idea about this kind of complex is their weak bonding strength with small intermolecular charge redistribution. It seems that in most previous interpretations, if the electrostatic interaction is regarded as the principle origin for the intermolecular bonding, then the charge-transfer effect cannot be the dominant factor for describing the bonding nature. However, there is no ground to show that the electrostatic interaction is contradictory to the CT effect. Actually, they can be concerted under a certain circumstance. For example, the electrostatic interaction is the main mechanism for the ionic compound where charge transfer is bound to happen during the formation.

Better alternative theoretical approaches may be used to study the bonding nature. Since  $\psi_N$  has both covalent and ionic bonding components, these two factors for determining the complex's properties should be considered at the same time. Different molecular systems may have different weights for these two factors. As we know, in a covalent bond, when

<sup>⊗</sup> Abstract published in *Advance ACS Abstracts*, March 15, 1997.

**TABLE 1: Geometries, Dipole Moments, and Energies of Monomers<sup>d</sup>**

compound	calcd (Å, deg) <sup>a</sup>	calcd (Å, deg) <sup>b</sup>	exptl (Å, deg) <sup>c</sup>	$\mu_{\text{calcd}}$ (D) <sup>a</sup>	$\mu_{\text{calcd}}$ (D) <sup>b</sup>	$\mu_{\text{exp}}$ (D) <sup>c</sup>	<i>E</i> (au)
NH <sub>3</sub>	1.009,107.69	1.015,106.83	1.012,106.7	1.77	1.85	1.47	-11.665 81
HF	0.914	0.919	0.917	2.03	2.09	1.83	-24.732 33
HCl	1.289	1.286	1.275	1.38	1.43	1.11	-15.468 88
HBr	1.415	1.414	1.415	1.06	1.10	0.83	-13.935 19
HI	1.601	1.600	1.609	0.68	0.69	0.45	-11.991 49
ClF	1.650	1.682	1.628	1.24	1.50	0.89	-38.907 80
BrF	1.768	1.802	1.759	1.82	2.19	1.42	-37.394 98
IF	1.924	1.961		2.47	2.93	1.95	-35.477 74
BrCl	2.158	2.167	2.136	0.57	0.70	0.52	-28.179 87
ICl	2.335	2.346	2.321	1.29	1.51	1.24	-26.255 13
IBr	2.484	2.498	2.469	0.75	0.88	0.73	-24.732 29
F <sub>2</sub>	1.368	1.419	1.412				-48.083 10
Cl <sub>2</sub>	2.027	2.035	1.988				-29.698 43
Br <sub>2</sub>	2.297	2.309	2.281				-26.659 22
I <sub>2</sub>	2.681	2.695	2.666				-22.802 67

<sup>a</sup> Optimized with BHandHLYP. <sup>b</sup> Optimized with MP2. <sup>c</sup> Reference 46. <sup>d</sup> The listed structural parameters are the bond length and bond angle for NH<sub>3</sub> and bond lengths for others. The dipole moments of F<sub>2</sub>, Cl<sub>2</sub>, Br<sub>2</sub>, and I<sub>2</sub> are zero.

electrons delocalize from bonding atoms to the bonding area rather than directly transfer to counterpart bonding atoms, the electron cloud overlap is increased. Then the resultant bond must become more intensive, whereas in an ionic bond, electrons tend to transfer to bonding atoms because this kind of localization can augment the formal charges of bonding atoms. As a consequence, the electrostatic interaction is enlarged, which contributes to the resultant strong bonding strength. In this way, large charge-transfer extent is associated with large binding energy in the case of the ionic bond but with small binding energy in the case of the covalent bond. Therefore, the charge-transfer effect is important for both covalent and ionic bonding intensity but with opposite correlation.

There is no systematic experimental or theoretical study on the title gas-phase complexes and few interpretations of their intermolecular interaction concerning the consistent effects of the relevant tendency of the binding energy, the intermolecular stretching force constant, the charge-transfer extent, and the dipole moment. Hence, the current work is desired to utilize efficient theoretical tools to explain and predict structures, bondings, and properties of all complexes in the title series.

## II. Quantum Chemical Method

For the high-level theoretical work *ab initio* methods<sup>14</sup> are usually employed. Recently, the density functional theory (DFT),<sup>15–20</sup> because of its cost-efficient procedure in the research of ground-state molecular physical properties, has been developed very quickly and utilized in more and more theoretical investigations. Many functionals have been proposed.<sup>21–34</sup> Generally, the functional can be separated into exchange and correlation parts. There are two alternative treatments for the exchange part: Slater (S) type<sup>23</sup> and Becke (B) type.<sup>31</sup> In later calculations, the denotation Null means the correlation part is neglected. If it cannot be ignored, VWN,<sup>25</sup> P81,<sup>26</sup> P86,<sup>29</sup> and LYP<sup>33</sup> parametrizations can be employed. They have been implemented in the presently used *Gaussian 92* software.<sup>35,36</sup>

On the other hand, it has been found<sup>37–39</sup> that the ground-state molecular properties produced by the hybrid HF-DFT treatment are remarkably accurate. There are three kinds of hybrid HF-DFT treatment in *Gaussian 92*: Becke3P86, Becke3LYP, and BHandHLYP. The DFT part in Becke3P86 is B-VWN-P86. Although the DFT part in both Becke3LYP and BHandHLYP is B-LYP, HandH in the latter term means half Hartree–Fock exchange and half Slater exchange.<sup>40</sup> Actually, many DFT methods have already been found to be good choices in the study of some hydrogen-bonded supramolecular

systems.<sup>41,42</sup> In this paper, the hybrid HF-DFT method BHandHLYP was adopted.

Since the title complexes includes heavy atoms, the compact effective potentials (CEP-121G)<sup>43</sup> for H, N, F, and Cl and relativistic compact effective potentials (RCEP)<sup>44</sup> for Br and I were adopted here. A d-type polarization function for each nonhydrogen atom and a p-type polarization function for the hydrogen atom have been augmented. The d orbital exponents, 0.864, 1.496, 0.514, 0.389, and 0.266 for N, F, Cl, Br, and I, respectively, were from ref 45.

In all calculations, the symmetry of the complex is kept as *C*<sub>3v</sub> according to some experimental and theoretical results.<sup>1–5</sup> The orientation of component atoms in the complex was taken as H<sub>3</sub>N·HX, H<sub>3</sub>N·XY, and H<sub>3</sub>N·X<sub>2</sub>, in which the electronegativity of halogen Y is larger than that of halogen X.<sup>1–5</sup> *Direct* SCF technique was used in the optimizations for both component molecules and supermolecules except for the complex H<sub>3</sub>N·I<sub>2</sub>, where the *quadratic convergent* (QC) method was utilized to resolve the convergence problem.

## III. Equilibrium Structures of Component Molecules and Complexes

The equilibrium structures of all component molecules are listed in Table 1. It can be seen that the difference of each bond length from the experimental value is small in the case of the hybrid HF-DFT method BHandHLYP. Such difference falls within 0.000–0.044 Å for all monomers. The average difference is only 0.016 Å. These results are better than those obtained by the MP2 method with the same basis sets because the mean difference in the latter case is 0.023 Å. The largest difference is 0.054 Å among MP2 results, which is greater than that among BHandHLYP results. The difference between the calculated bond angle ∠H–N–H and the experimental one by BHandHLYP is not large, merely 0.99°. In addition, the dipole moments of monomers produced by BHandHLYP are more close to experimental data than those produced by MP2. The mean differences of the dipole moment from the experimental measurement are 0.24 and 0.41 D in the case of BHandHLYP and MP2, respectively. In fact, the linear correlation coefficient for the relationship between the calculated (with BHandHLYP) and experimental dipole moments is as high as 0.99. These facts show the effectiveness and accuracy of the uses of the hybrid HF-DFT method and the associated CEP121G(d,p) and RCEP(d) basis sets. Actually, BHandHLYP is selected because it seems to be the best quantum chemical method among DFT and hybrid HF-DFT methods of the presently used *Gaussian*

TABLE 2: Selected Optimized Parameters

method	exptl <sup>a</sup>	HF	MP2	B-Null	B-P81	B-P86	B-VWN	B-LYP	Becke3LYP	Becke3P86	BHandHLYP
$R_{\text{Br-Cl}}$	2.136	2.142	2.167	2.262	2.226	2.194	2.221	2.219	2.188	2.169	2.158
$R_{\text{H-F}}$	0.917	0.901	0.919	0.945	0.933	0.933	0.932	0.937	0.926	0.923	0.914
$\mu_{\text{BrCl}}$	0.52	0.66	0.70	0.48	0.51	0.47	0.51	0.49	0.52	0.51	0.57
$\mu_{\text{HF}}$	1.83	2.06	2.09	1.94	1.95	1.98	1.95	1.96	2.00	2.01	2.03

<sup>a</sup> Reference 46.

TABLE 3: Geometries, Energies, and Force Constants of the Title Complexes

compound	$R_{\text{A-B}}$ (Å)	$R_{\text{N-A(B)}}$ (Å)	$E$ (au)	$E_{\text{B}}$ (kcal/mol)	$k_{\text{cal}}$ (N/m)	$k_{\text{exp}}$ (N/m)
$\text{H}_3\text{N}\cdot\text{HF}$	0.945	2.638	-36.422 50	15.29	47.93	32.8 <sup>a</sup>
$\text{H}_3\text{N}\cdot\text{HCl}$	1.344	3.077	-27.152 27	11.03	32.52	18.2 <sup>b</sup>
$\text{H}_3\text{N}\cdot\text{HBr}$	1.482	3.209	-25.616 37	9.64	27.70	13.4 <sup>a</sup>
$\text{H}_3\text{N}\cdot\text{HI}$	1.669	3.447	-23.668 90	7.28	18.80	
$\text{H}_3\text{N}\cdot\text{ClF}$	1.703	2.346	-50.593 81	12.68	43.47	
$\text{H}_3\text{N}\cdot\text{BrF}$	1.825	2.372	-49.088 78	17.56	57.19	
$\text{H}_3\text{N}\cdot\text{IF}$	1.973	2.520	-47.175 21	19.87	57.19	
$\text{H}_3\text{N}\cdot\text{BrCl}$	2.212	2.523	-39.863 21	11.00	37.56	26.8 <sup>c</sup>
$\text{H}_3\text{N}\cdot\text{ICl}$	2.392	2.625	-37.943 61	14.23	42.84	
$\text{H}_3\text{N}\cdot\text{IBr}$	2.540	2.663	-36.418 01	12.49	36.17	
$\text{H}_3\text{N}\cdot\text{F}_2$	1.383	2.585	-59.751 64	1.71	7.43	
$\text{H}_3\text{N}\cdot\text{Cl}_2$	2.066	2.566	-41.374 38	6.36	22.45	12.7 <sup>d</sup>
$\text{H}_3\text{N}\cdot\text{Br}_2$	2.347	2.574	-38.339 59	9.14	33.14	18.5 <sup>c</sup>
$\text{H}_3\text{N}\cdot\text{I}_2$	2.730	2.737	-34.484 25	9.90	34.63	

<sup>a</sup> Reference 1. <sup>b</sup> Reference 48. <sup>c</sup> Reference 4. <sup>d</sup> Reference 5.

92 software as exemplified in Table 2. The results from the *ab initio* HF and MP2 methods are presented for comparison. For the nonheavy-atom-containing molecule hydrogen fluoride, the geometry from BHandHLYP is much more favorable than others except for MP2. As regards to the heavy-atom-containing species, such as BrCl, its geometry is also much better than others except for the HF method. But in both cases, the dipole moments generated from BHandHLYP are better than those from HF and MP2. As we know, the lengthening of the bond lengths will result in the reduced dipole moments for these diatomic molecules. Since the bond lengths calculated by other DFT methods are longer than that by BHandHLYP, the dipole moments by other DFT functionals are smaller. In this way, they are seemingly more close to the experimental data.

The theoretical prediction of the complexes' equilibrium structures are illustrated in Table 3.  $R_{\text{N}\cdots\text{A(B)}}$  is the intermolecular distance between nitrogen and the nearest halogen, i.e., between N and X in the case of  $\text{H}_3\text{N}\cdot\text{HX}$ , between N and X in the case of  $\text{H}_3\text{N}\cdot\text{XY}$ , and between N and X(1) in the case of  $\text{H}_3\text{N}\cdot\text{X}(1)-\text{X}(2)$ .

It can be seen that, for instance, the bond length of BrCl in the complex is lengthened to 2.212 Å. This value is a bit larger by 0.026 Å than the experimental one.<sup>4</sup> The intermolecular distance between nitrogen and bromine is a little shorter by 0.068 Å than the experimental measurement. The predicted bond length of BrCl after the formation of the complex is lengthened by 0.054 Å, which is comparable to the measured lengthening of 0.047 Å.<sup>4</sup> Moreover, predictions of the important structural parameters by the hybrid HF-DFT method in this work are better than those in some *ab initio* work. For example, the experimental intermolecular distance  $\text{N}\cdots\text{X}$  for  $\text{H}_3\text{N}\cdot\text{HCl}$ <sup>5</sup> and  $\text{H}_3\text{N}\cdot\text{HBr}$ <sup>1</sup> are 3.136 and 3.255 Å, respectively. The differences between the experimental data and the large-scale *ab initio* results<sup>12</sup> are 0.134 and 0.125 Å, which are 2 or 3 times as large as the differences between the experimental results and our predictions, 0.059 and 0.046 Å, respectively. These results further prove the accuracy of current quantum chemical method.

As regards to the structural change of the common subunit  $\text{NH}_3$ , the bond length of nitrogen-hydrogen after the formation

of the complex does not change except for a tiny lengthening of 0.001 Å in the cases of HX, IF, ICl, and IBr involved. The bond angle variation falls within a small range of 0.12–1.05°. It is evident that the ammonia molecule is just a little compressed in the complex, in accordance with the weak intermolecular bonding character.

On the other hand, the bond length change of the halogen-containing subunit is greater than that of ammonia as exemplified by Tables 1 and 3, which indicates that the halogen-containing subsystem is more affected in the complex formation. All the component molecules of this subunit are lengthened in the range 0.015–0.068 Å.

The optimized values for the intermolecular distance are a bit shorter compared with some experimental results (i.e., 2.638 *vs* 2.710 Å for  $R_{\text{N}\cdots\text{F}}$  in  $\text{H}_3\text{N}\cdot\text{HF}$ ,<sup>1</sup> 3.077 *vs* 3.136 Å for  $R_{\text{N}\cdots\text{Cl}}$  in  $\text{H}_3\text{N}\cdot\text{HCl}$ ,<sup>5</sup> 3.209 *vs* 3.255 Å for  $R_{\text{N}\cdots\text{Br}}$  in  $\text{H}_3\text{N}\cdot\text{HBr}$ ,<sup>1</sup> and 2.523 *vs* 2.591 Å for  $R_{\text{N}\cdots\text{Br}}$  in  $\text{H}_3\text{N}\cdot\text{BrCl}$ <sup>4</sup>). This shortening effect may be systematically transferred to the little overestimation of the interaction strength in the following studies.

#### IV. Evaluation of the Binding Energy

The binding energy  $E_{\text{B}}$  is important in the study of the bonding strength. It can be regarded as the energy difference between the complex and the monomers:

$$E_{\text{B}} = E(\text{NH}_3) + E(\text{AB}) - E(\text{H}_3\text{N}\cdot\text{AB}) \quad (2)$$

As shown in Table 3, the binding energy ranges from 1.71 to 19.87 kcal/mol. These quantities cannot be regarded as large compared to the ordinary chemical bond. The relative order of these energies is the same as computed by other theoretical work for some CT complexes among the title series.<sup>11,12</sup>

As for the hydrogen-bonded complexes  $\text{H}_3\text{N}\cdot\text{HX}$ , the binding energies are similar to other hydrogen-bonding energies. It can be seen from Table 3 that  $E_{\text{B}}$  decreases with the decrease of the halogen's electronegativity, i.e., with the decrease of the difference between the nitrogen atom's and the halogen atom's electronegativities. This fact is in agreement with common chemical intuition about the hydrogen bonding. It is known that in the usual covalent bond formed by heteroatoms, its stability increases with increasing difference between the two component atom's electronegativities, such as  $E_{\text{B}}(\text{HF}) > E_{\text{B}}(\text{HCl}) > E_{\text{B}}(\text{HBr}) > E_{\text{B}}(\text{HI})$ , which is the same as the relative order of the hydrogen-bonding energies of current complexes. So the covalent part  $\psi_0(\text{D,A})$  may be dominant in describing the hydrogen-bonded complex's properties.

As demonstrated in Table 3, the stability of the complex formed with XY or X<sub>2</sub> increases with the increase of the atomic number. The heteronuclear molecules form more stable complexes than homonuclear molecules. These phenomena were also observed in experimentations.<sup>47</sup> With the general form  $\text{H}_3\text{N}\cdot\text{AB}$ , it can be found that if atom B is fixed, the stability increases with increasing radius and decreasing electronegativity of atom A. For instance, the binding energies of  $\text{H}_3\text{N}\cdot\text{F}_2$ ,  $\text{H}_3\text{N}\cdot\text{ClF}$ ,  $\text{H}_3\text{N}\cdot\text{BrF}$ , and  $\text{H}_3\text{N}\cdot\text{IF}$  are 1.71, 12.68, 17.56, and 19.87 kcal/mol, respectively. This feature is opposite to the relation of the above hydrogen-bonding systems. On the other hand, if

atom A is fixed, the stability increases with the increasing electronegativity of atom B. This may be accounted for by the increasing inductive effect of atom B upon atom A. In this way, atom A has more charges to maintain strong electrostatic interaction. It can be exemplified by the binding energies of  $\text{H}_3\text{N}\cdot\text{I}_2$ ,  $\text{H}_3\text{N}\cdot\text{IBr}$ ,  $\text{H}_3\text{N}\cdot\text{ICl}$ , and  $\text{H}_3\text{N}\cdot\text{IF}$  as 9.90, 12.49, 14.23, and 19.87 kcal/mol, respectively. The formal charges of atom A in this series, 0.072, 0.135, 0.220, and 0.369 e (see Table 4 later), respectively, can indicate the presence of the inductive effect. As a consequence, the experimentally suggested electrostatic origin<sup>4</sup> can find the theoretical ground here. Therefore, the ionic part  $\psi_1(\text{D}^+-\text{A}^-)$  may be the principal component of its ground-state wave function in this case.

### V. Intermolecular Stretching Force Constant

The intermolecular stretching force constant,  $k$ , is also important in the investigation of the intermolecular bonding strength.

There is no analytical calculation available to obtain the force constant in the *Gaussian 92* software in the case of the CEP basis set used. At the same time, the numerical calculation of all the complexes is very time-consuming because of the limitation of our available computer resources. Therefore, an efficient alternative approach should be sought out to estimate the value of  $k$ .

Generally, the total energy for a given system  $E$  near the equilibrium geometry can be approximately described as follows:

$$E = k(r - r_e)^2 / (2 + E_e) \quad (3)$$

where  $E_e$  denotes the total energy of the system at the equilibrium geometry,  $r$  is the intermolecular distance between the two subsystems of the complex, and  $r_e$  is that distance at the equilibrium geometry. Thus, the intermolecular stretching force constant can be calculated if other quantities are known. In order to increase the accuracy of the computation, many data sets should be used. Then the parabolic fit procedure was performed to get the optimal value for the intermolecular stretching force constant. All these quantities obtained in this way are listed in Table 3.

In order to verify the efficiency of this method, some available experimental data as shown in Table 3 are used for comparison. It can be seen that the overestimation is present in all complexes listed here because of the underestimation of the intermolecular distance as discussed in the previous part. But such overestimation is systematic and consistent because there is an excellent linear relationship with the correlation coefficient 0.97 between the calculated ( $k_{\text{cal}}$ ) and the experimental ( $k_{\text{exp}}$ ) force constants. This fact, as illustrated in Figure 1, shows that theoretical results parallel results from experimental measurements.

The excellent consistency of the present theoretical investigation can also be exemplified by the parallel relationship between the calculated binding energy and the intermolecular stretching force constant for all the title complexes. Large binding energy means that the binding force between the component molecules of the complex is strong. Thus, the intermolecular stretching force constant must be large as well. The linear correlation coefficient for such a relation in Figure 2 is 0.98. Owing to the efficiency and consistency, the current approach may also be applied to predict the intermolecular stretching force constants for such species where the experimental data are unavailable now.

### VI. Intra- and Intermolecular Charge Transfer

The step-by-step charge-transfer (SBSCT) model was suggested here to approximately estimate these two quantities by

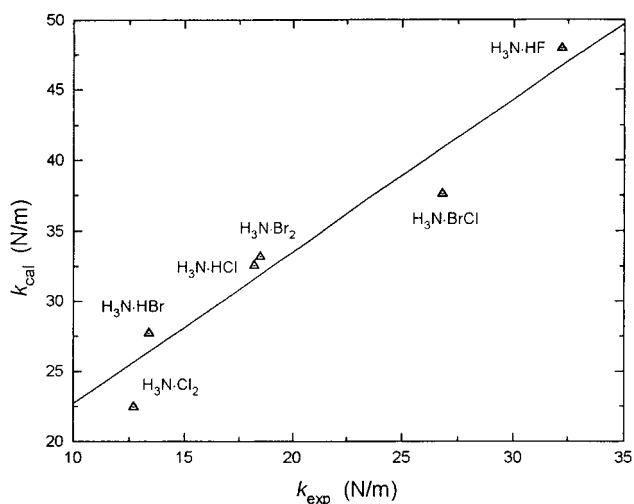


Figure 1. Plot of the calculated *vs* experimental force constant.

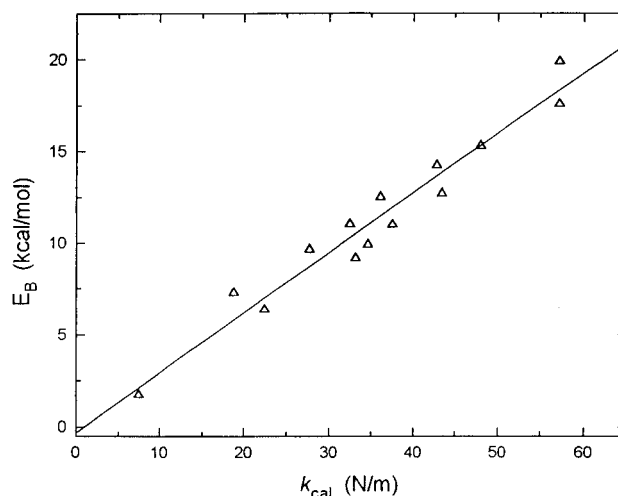


Figure 2. Plot of the binding energy *vs* the calculated force constant.

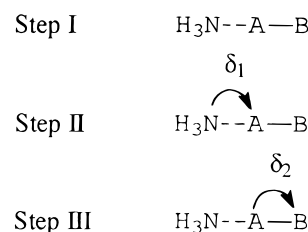


Figure 3. Step-by-step charge-transfer model.

the example of the complex  $\text{H}_3\text{N}\cdot\text{AB}$ . At the equilibrium geometry, the formal charges of atom A and B in the component molecule and the complex are written as  $q$ ,  $-q$  and  $Q_A$ ,  $-Q_B$ , respectively. Here, these physical quantities ( $q$ ,  $Q_A$ , and  $Q_B$ ) are non-negative because the electronegativity of element B is not less than that of element A.

As illustrated in Figure 3, in the first step, the two subunits come together to reach the equilibrium geometry, but no charge has been transferred. So now molecule AB is still neutral, i.e., the formal charges of atoms A and B must also be equivalent to  $q$  and  $-q$ , respectively. In the following two steps, the equilibrium structure is kept unchanged, but the charge redistribution takes place to stabilize the complex. In the second step, it is assumed that the amount ( $\delta_1$ ) of total intermolecular charge transfer happens from the subunit  $\text{NH}_3$  to atom A, for atom A is adjacent to the subunit ammonia. If this is true,  $\delta_1$  must be positive; otherwise the negative value of  $\delta_1$  means the opposite charge-transfer direction. So after this step, there is

TABLE 4: Charge-Transfer Extents and Dipole Moments of the Title Complexes

compound	$q$ (e)	$Q_A$ (e)	$Q_B$ (e)	$\delta_1$ (e)	$\delta_2$ (e)	$\mu$ (D)	$\mu'$ (D)	$\Delta\mu$ (D)	$\chi_\mu$ (%)
H <sub>3</sub> N•HF	0.391	0.399	0.461	0.062	0.070	4.93	3.85	1.08	21.9
H <sub>3</sub> N•HCl	0.243	0.292	0.380	0.088	0.137	5.03	3.18	1.85	36.8
H <sub>3</sub> N•HBr	0.146	0.193	0.299	0.106	0.153	5.10	2.83	2.27	44.5
H <sub>3</sub> N•HI	0.079	0.171	0.269	0.098	0.190	4.92	2.41	2.51	51.0
H <sub>3</sub> N•ClF	0.215	0.232	0.334	0.102	0.119	5.63	3.09	2.54	45.1
H <sub>3</sub> N•BrF	0.305	0.290	0.419	0.129	0.114	6.79	3.72	3.07	45.2
H <sub>3</sub> N•IF	0.408	0.369	0.500	0.131	0.092	7.57	4.39	3.18	42.0
H <sub>3</sub> N•BrCl	0.090	0.141	0.246	0.105	0.237	5.52	2.34	3.18	57.6
H <sub>3</sub> N•ICl	0.173	0.220	0.332	0.112	0.159	6.69	3.14	3.55	53.1
H <sub>3</sub> N•IBr	0.080	0.135	0.247	0.112	0.167	6.38	2.55	3.83	60.0
H <sub>3</sub> N•F <sub>2</sub>	0.000	0.029	0.046	0.017	0.046	2.35	1.76	0.59	25.1
H <sub>3</sub> N•Cl <sub>2</sub>	0.000	0.071	0.131	0.060	0.131	3.97	1.73	2.24	56.4
H <sub>3</sub> N•Br <sub>2</sub>	0.000	0.052	0.156	0.104	0.156	5.02	1.71	3.31	65.9
H <sub>3</sub> N•I <sub>2</sub>	0.000	0.072	0.173	0.101	0.173	5.52	1.73	3.79	68.7

no net intermolecular charge transfer between two monomers. Now the formal charge of atom A ( $q_A'$ ) is equal to  $q - \delta_1$ . Because atom B is not involved in this step, its formal charge ( $-q_B'$ ) must be the same as ( $-q$ ). But the intermolecular charge transfer should take place between two subsystems rather than between one subsystem NH<sub>3</sub> and one part (atom A) of the other subsystem. So atom A usually cannot sustain all the intermolecular charge gain (when  $\delta_1$  is positive) or loss (when  $\delta_1$  is negative). Then the intramolecular charge redistribution of the subunit AB is necessary to reach the real circumstance of the resultant complex. In the third step, the intramolecular charge transfer,  $\delta_2$ , is bound to happen from atom A to atom B. It is similar in that negative  $\delta_2$  means the opposite charge-transfer orientation.

After these three steps, the geometry and charge distribution are the same as in the complex. Therefore,  $Q_A$  is equal to  $q_A' + \delta_2$ , and ( $-Q_B$ ) is equal to ( $-q_B'$ ) -  $\delta_2$ . From these relations, the intra- and intermolecular charge transfer extent,  $\delta_1$  and  $\delta_2$ , can be deduced as follows:

$$\delta_1 = Q_B - Q_A \quad (4)$$

$$\delta_2 = Q_B - q \quad (5)$$

All these values are listed in Table 4. It can be seen that all of them are positive, which is in favor of the assumed CT direction introduced in the deduction of the above formulas. So in the complex H<sub>3</sub>N•AB, ammonia is the donor and molecule AB is the acceptor, which is in accordance with common chemical experience.

The amounts of both inter- and intramolecular charge transfer calculated here are very small. The largest values of  $\delta_1$  and  $\delta_2$  are 0.131 and 0.237 e, respectively. Such a small extent of the charge transfer is in agreement with both experimental and other theoretical conclusions as shown in the Introduction.

There are some regular trends of the charge-transfer extent. As regards to the relationship of  $\delta_1$  and  $E_B$  for the hydrogen-bonded complexes, it follows this tendency:  $E_B$  generally increases with decreasing  $\delta_1$ . This phenomenon is similar to the charge-transfer effect on the covalent bond introduced previously, which again suggests the dominant importance of the covalent wave function  $\psi_0(D,A)$  for this series of complexes. For the complexes H<sub>3</sub>N•XY and H<sub>3</sub>N•X<sub>2</sub>,  $E_B$  generally increases with the increase of  $\delta_1$ . The correlation coefficient of the linear relationship between  $\delta_1$  and  $E_s$  is 0.92, and that value for  $\delta_1$  and  $k$  is even better at 0.94. The latter relation is demonstrated in Figure 4. This kind of relationship is similar to the behavior of ionic bonding, which again suggests the relative significance of the ionic character compared with the covalent part in the total ground-state wave function. These good relationships indicate that, though the absolute value of the intermolecular

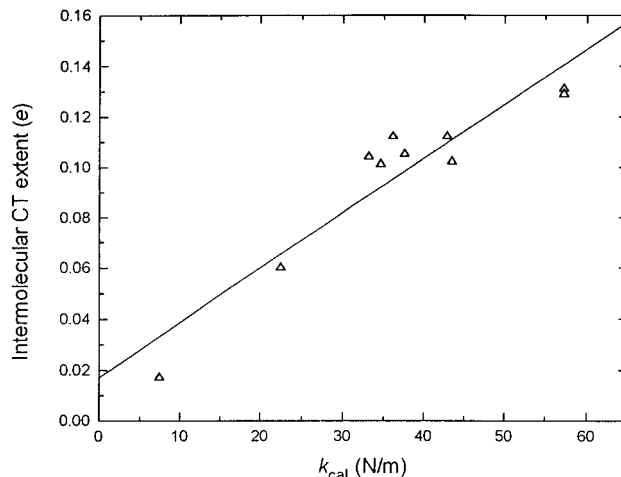


Figure 4. Plot of the intermolecular CT extent *vs* calculated force constant.

charge transfer is small, the CT effect is still the important factor in determining the bonding strength for all the discussed complexes.

It is found that the complex generally becomes more stable with the decrease of  $\delta_2$  so as to maintain the ordinary covalent bond A-B. For the hydrogen-bonded systems H<sub>3</sub>N•HX, because the hydrogen atom is usually unable to contain the charges transferred from the nitrogen atom, it soon releases them to the much more electronegative halogen atom. Therefore, when  $\delta_1$  increases,  $\delta_2$  generally increases as well. However, for other complexes, H<sub>3</sub>N•AB (AB = XY and X<sub>2</sub>), if atom B is fixed,  $\delta_1$  becomes larger with the increasing radius of atom A to benefit the electrostatic interaction because an atom with a large radius can be easily polarized. At the same time,  $\delta_2$  is usually decreased with the increase of the atomic number to make atom A maintain enough electric charge for the electrostatic interaction except that  $\delta_2$  of H<sub>3</sub>N•X<sub>2</sub> is the smallest among such a series. For example,  $\delta_1$  and  $\delta_2$  for H<sub>3</sub>N•F<sub>2</sub>, H<sub>3</sub>N•ClF, H<sub>3</sub>N•BrF, and H<sub>3</sub>N•IF are (0.017, 0.046), (0.102, 0.119), (0.129, 0.114), and (0.131, 0.092) e, respectively. Here, the intramolecular CT extent for H<sub>3</sub>N•F<sub>2</sub> is the smallest among the four complexes, which may be due to the fact that this is needed to keep the stable covalent bond of F<sub>2</sub> after the formation of the complex compared with others. This kind of relation can also be found in other series, i.e., (1) H<sub>3</sub>N•Cl<sub>2</sub>, H<sub>3</sub>N•BrCl, H<sub>3</sub>N•ICl and (2) H<sub>3</sub>N•Br<sub>2</sub>, H<sub>3</sub>N•IBr. In the case where atom A is fixed,  $\delta_1$  is increased with increasing electronegativity of atom B through the inductive effect, which is accompanied by a decreasing  $\delta_2$  to stabilize the original covalent bond of the halogen-containing part. It can be exemplified by the inter- and intramolecular CT amounts of H<sub>3</sub>N•I<sub>2</sub>, H<sub>3</sub>N•IBr, H<sub>3</sub>N•ICl, and H<sub>3</sub>N•IF as (0.101, 0.173), (0.112, 0.167), (0.112, 0.159),

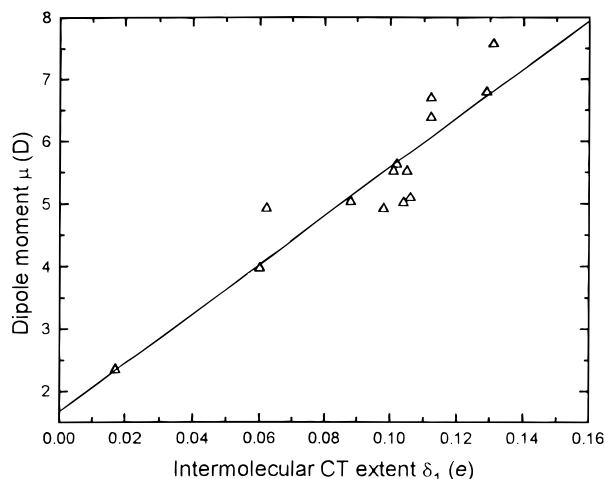


Figure 5. Plot of the dipole moment *vs* intermolecular CT extent.

and (0.131, 0.092) e, respectively. All these clear and regular relations further prove the present conclusion of their intermolecular bonding nature.

### VII. Dipole Moment and Quantitative Evaluation of Covalent and Ionic Character

The dipole moments of all complexes are listed in Table 4. It can be seen that the magnitude of the dipole moment changes accordingly with the intermolecular charge transfer extent. As illustrated in Figure 5, the good relationship between  $\delta_1$  and  $\mu$  can be evidenced by the linear correlation coefficient of 0.92. Such a relationship shows that the CT effect is the dominant factor in determining the complex's dipole moment. Therefore, the discussion of the CT effect on the intermolecular bonding strength in the former part can be applied to the dipole moment as well.

In order to quantitatively evaluate the weights of the covalent (or nonelectrostatic) and the ionic (or electrostatic) contributions to the complex stabilization, we may take advantage of the dipole moment variation. If the intermolecular bonding is purely nonelectrostatic, the dipole moment of the complex is expected to be the vector sum of the dipole moments of both subunits in the complex geometry. As shown in Table 4, this quantity,  $\mu'$ , is not equal to  $\mu$  in all cases. The difference between these two values, defined as  $\Delta\mu$  in Table 4, can be regarded as a consequence of the electrostatic contribution.  $\chi_\mu$  represents the percentage variation of the dipole moment, i.e.,  $\Delta\mu/\mu \times 100\%$ . It can be seen that the electrostatic contribution increases with decreasing electronegativity of the halogen. For instance, both  $\Delta\mu$  and  $\chi_\mu$  increase in the order of  $F < Cl < Br < I$  in hydrogen-bonded complexes,  $H_3N \cdot AB$ , the same trend can be found no matter if A or B is fixed, such as ( $H_3N \cdot F_2$ ,  $H_3N \cdot ClF$ ,  $H_3N \cdot BrF$ ,  $H_3N \cdot IF$ ) and ( $H_3N \cdot IF$ ,  $H_3N \cdot ICl$ ,  $H_3N \cdot IBr$ ,  $H_3N \cdot I_2$ ). This phenomenon was also indicated by other theoretical work<sup>42</sup> on  $H_2O \cdot HF$  and  $H_2O \cdot HCl$ .

The  $\Delta\mu$  and  $\chi_\mu$  of hydrogen-bonded complexes are generally not large, which indicates that the covalent character is more significant than the ionic one. But they are large in  $H_3N \cdot XY$  and  $H_3N \cdot X_2$ , which suggests that the ionic character is more important than the covalent one. These facts are in agreement with the previous discussion. However, these two quantities can be used for a more accurate interpretation of intermolecular bonding. For example, on account of the increase of the ionic character in  $H_3N \cdot HI$ ,  $\delta_1$  decreases rather than increases with  $E_B$  as in other hydrogen-bonded complexes.

### VIII. Conclusions

Based on above discussions, the hybrid HF-DFT method BHandHLYP together with the combined use of the CEP-121G-(d,p) for the first- and second-row elements and RCEP for the third- and fourth-row elements are good choices for the efficient study of weakly bonded CT complexes. The intermolecular stretching force constant derived from the parabolic fit of the energy curve parallels the experimental results. There is a good consistency between the calculated  $k$  and  $E_B$ . The SBSCT model, though simple in formalism, is capable of producing the direct estimation of both intra- and intermolecular charge-transfer extent, which contributes to the reasonable explanation of the bondings of the title complexes. The intermolecular CT amount is not large. But the CT effect has been found to be significant in determining the bonding strength. The intensity of the intermolecular bonding for the hydrogen-bonded complexes  $H_3N \cdot HX$  decreases with its intermolecular CT amount, while the opposite relation exists for other complexes. The  $\Delta\mu$  and  $\chi_\mu$  of the complex can be utilized in the quantitative estimation of the ionic or electrostatic contribution to the complex's stabilization. The effectiveness, accuracy, and consistency of the present work make it possible to predict some properties of unknown complexes in this area.

**Acknowledgment.** Thanks to the financial support of State Science and Technology Commission and the National Natural Science Foundation of China for this work.

### References and Notes

- (1) Howard, N. W.; Legon, A. C. *J. Chem. Phys.* **1987**, *86*, 6722.
- (2) Legon, A. C.; Millen, D. J. *Chem. Phys. Lett.* **1988**, *147*, 484.
- (3) Kobayashi, T.; Matsuzawa, H.; Iwata, S. *Bull. Chem. Soc. Jpn.* **1994**, *67*, 3172.
- (4) Bloemink, H. I.; Legon, A. C.; Thorn, J. C. *J. Chem. Soc., Faraday Trans.* **1994**, *90*, 781.
- (5) Bloemink, H. I.; Hinds, K.; Legon, A. C.; Thorn, J. C. *Chem. Phys. Lett.* **1994**, *223*, 162.
- (6) Millen, D. J. *Can. J. Chem.* **1985**, *63*, 1477.
- (7) Mulliken, R. S.; Person, W. B. In *Molecular Complexes*; Wiley-Interscience: New York, 1969.
- (8) Mulliken, S. R. *J. Am. Chem. Soc.* **1952**, *74*, 811.
- (9) Mulliken, R. S.; Person, W. B. *J. Am. Chem. Soc.* **1969**, *91*, 3409.
- (10) Hanna, M. W.; Lippert, J. L. In *Molecular Complexes*; Foster, R., Ed.; Elek: London, 1973; Vol. 1.
- (11) Røeggen, I.; Dahl, T. *J. Am. Chem. Soc.* **1992**, *114*, 511.
- (12) Brciz, A.; Karpfen, A.; Lischka, H.; Schuster, P. *Chem. Phys.* **1984**, *89*, 337.
- (13) Reed, A. E.; Weinbold, F.; Curtiss, L. A.; Pochatko, D. J. *J. Chem. Phys.* **1986**, *84*, 5687.
- (14) Hehre, W. J.; Radom, L.; Schleyer, P. v. R.; Pople, J. A. In *Ab Initio Molecular Orbital Theory*; John Wiley & Sons: New York, 1986.
- (15) Hohenberg, P.; Kohn, W. *Phys. Rev. B* **1964**, *136*, 864.
- (16) Kohn, W.; Sham, L. J. *Phys. Rev. A* **1965**, *140*, 1133.
- (17) Jones, R. O.; Gunnarsson, O. *Rev. Mod. Phys.* **1989**, *61*, 689.
- (18) Parr, R. G.; Yang, W. In *Density-Functional Theory of Atoms and Molecules*; Oxford University Press: New York, 1989.
- (19) Ziegler, T. *Chem. Rev.* **1991**, *91*, 651.
- (20) In *Density Functional Methods in Chemistry*; Labanowski, J. K., Andzelm, J., Eds.; Springer-Verlag: New York, 1991.
- (21) Wigner, E. P. *Trans. Faraday Soc.* **1938**, *34*, 678.
- (22) Herman, F.; Van Dyke, J. P.; Ortenburger, I. B. *Phys. Rev. Lett.* **1969**, *22*, 807.
- (23) Slater, J. C. In *Quantum Theory of Molecules and Solids, Vol. 4: The Self-Consistent Field for Molecules and Solids*; McGraw-Hill: New York, 1974.
- (24) Brual, G., Jr.; Rothstein, S. M. *J. Chem. Phys.* **1978**, *69*, 1177.
- (25) Vosko, S. H.; Wilk, L.; Nusair, M. *Can. J. Phys.* **1980**, *58*, 1200.
- (26) Perdew, J. P.; Zunger, A. *Phys. Rev. B* **1981**, *23*, 5048.
- (27) Becke, A. D. *J. Chem. Phys.* **1986**, *84*, 4524.
- (28) Ghosh, S. K.; Parr, R. G. *Phys. Rev. A* **1986**, *34*, 785.
- (29) Perdew, J. P. *Phys. Rev. B* **1986**, *33*, 8822.
- (30) Becke, A. D. *J. Chem. Phys.* **1988**, *88*, 1053.
- (31) Becke, A. D. *Phys. Rev. A* **1988**, *38*, 3098.
- (32) Cedillo, A.; Robles, J.; Gázquez, J. L. *Phys. Rev. A* **1988**, *38*, 1697.
- (33) Lee, C.; Yang, W.; Parr, R. G. *Phys. Rev. B* **1988**, *37*, 785.

- (34) Wilson, L. C.; Levy, M. *Phys. Rev. B* **1990**, *41*, 12930.
- (35) Johnson, B. G.; Gill, P. M. W.; Pople, J. A. *J. Chem. Phys.* **1993**, *98*, 5612.
- (36) Frisch, M. J.; Trucks, G. W.; Schlegel, H. B.; Gill, P. W.; Johnson, B. G.; Wong, M. W.; Foresman, J. B.; Robb, M. A.; Head-Gordon, M.; Replogle, E. S.; Gomperts, R.; Andres, J. L.; Raghavachari, K.; Binkley, J. S.; Gonzalez, C.; Martin, R. L.; Fox, D. J.; Defrees, D. J.; Baker, J.; Stewart, J. J. P.; Pople, J. A. *Gaussian 92/DFT*, Revision F.2; Gaussian Inc.: Pittsburgh, PA, 1993.
- (37) Gill, P. M. W.; Johnson, B. G.; Pople, J. A. *Chem. Phys. Lett.* **1992**, *197*, 499.
- (38) Scuseria, G. E. *J. Chem. Phys.* **1992**, *97*, 7528.
- (39) Oliphant, N.; Barlett, R. J. *J. Chem. Phys.* **1994**, *100*, 6550.
- (40) Becke, A. D. *J. Chem. Phys.* **1993**, *98*, 1372.
- (41) Latajka, Z.; Bouteiller, Y. *J. Chem. Phys.* **1994**, *101*, 9793.
- (42) Pérez, P.; Contreras, R. *Chem. Phys. Lett.* **1996**, *256*, 15.
- (43) Stevens, W. J.; Basch, H.; Krauss, M. *J. Chem. Phys.* **1984**, *81*, 6026.
- (44) Stevens, W. J.; Krauss, M. *Can. J. Chem.* **1992**, *70*, 612.
- (45) In *Physical Sciences Data 16: Gaussian Basis Set for Molecular Calculations*; Huzinaga, S., Ed.; Elsevier: Amsterdam, 1985.
- (46) In *CRC Handbook of Chemistry and Physics*, 73rd ed.; CRC Press: Boca Raton, FL, 1992.
- (47) Foster, R. In *Organic Charge-transfer Complexes*; Academic Press London: New York, 1969; p 201.
- (48) Legon, A. C.; Millen, D. J. *J. Am. Chem. Soc.* **1987**, *109*, 356.